59th ILMENAU SCIENTIFIC COLLOQUIUM
Technische Universität Ilmenau, 11 – 15 September 2017
URN: urn:nbn:de:gbv:ilm1-2017iwk-073:3

AUTOMATIC OPTIMIZATION OF LOAD ANGLES FOR A LINEAR HYBRID STEPPER MOTOR

H. Weiß, T. Bauer, M. Eichhorn

Technische Universität Ilmenau, Institute for Automation and Systems Engineering, System Analysis Group

ABSTRACT

The objective of this contribution is a linear direct drive based on the working principle of hybrid stepper technology. Herein, reluctant forces enable the thrust of this type of drive. In order to improve the dynamic performance a method adjusting the optimal load angle with respect to the driven velocity is presented.

Commonly, the phases of the linear hybrid stepper motor (LHSM) are commutated sinusoidal with a constant load angle of 90 degrees. Due to delay times of sensors, actuators and hardware, the coils of the phases are not energized optimally in terms of maximum force application. Thus, variable load angles subject to velocity are introduced.

This contribution comprises the optimization of the load angles. To solve this one-dimensional optimization task, bracketing methods can be used. These algorithms work without derivatives and find the minimum through iterative decreasing of the interval until a desired tolerance is achieved. Regarding the implementation, signal processing has to be done beside the optimization algorithm to ensure feasible solutions. The entire optimization process can be carried out automatically on the test rig. As a result, a characteristic curve is obtained describing the optimal load angle to velocity relation. Including the directionality, the characteristic curves are distinguished between forward and backward drive. Further properties of the optimization algorithm such as convergence and reproducibility are examined and discussed.

The curves are implemented on a real-time system facilitating a comparison with constant load angle commutation. Velocity control measurements exhibit an improved performance, especially at high motion dynamics.

Index Terms - Linear hybrid stepper motor, load angle, optimization, motion dynamics

1. INTRODUCTION

Linear hybrid stepper motors (LHSM) are deployed diversely in industry carrying out essential positioning tasks. Application fields cover metal machining, assembling and inspecting of manufactured parts and precision manufacturing [1]. Inherently, direct drives have no rotational-translational transducer such as belt or spindle drives. Thus, there are benefits over usual linear actuators concerning reduced component costs and less wear. Furthermore, dynamics deteriorating properties of transducers such as backlash and friction are avoided.

Formerly, the LHSM was deployed as a stepper motor capable of discrete positioning tasks in open loops. Simple hall sensors detected crudely the position allowing only switching the phase currents to discrete values in microstepping operation [2]. With the availability of high

resolution positioning signals and microprocessors, software-based commutation was applicable.

According to the motor design, the commutation can be specified to its characteristic back-EMF. Commonly, sinusoidal types are deployed due to better properties in general [3]. A corresponding sinusoidal commutation especially shows less force ripple as trapezoidal commutation. Since the back-EMF is assumed to be equal to the force constant [4], the peak value is at one quarter of commutation period. Thus, the control scheme of commutation is designed with a load angle of 90° for each phase. Because of mechanic tolerances the characteristic force constant function can be a shifted sinusoid and the maximum force application may not be available.

Additionally, the phase current energizes the coils with a time delay due to process latencies. These include delays of process components such as the position encoder and the cycle time of the real-time hardware. Moreover, plant characteristics concerning current and magnetic dynamics can produce delays occurring as time span from commanding the current to force application. Latencies of current dynamics arise by self-induction and velocity dependent back-EMF. In this context, the properties of the analog current amplifiers are essential. Within the magnetic domain, effects as eddy currents and hysteresis losses delay the rise of the magnetic flux. Since electric and magnetic time constants are in scale of milliseconds, it might be negligible. However, at high velocities of 1 m/s a position lag of 1 mm arises. Hence, the stated properties of the LHSM result in a thrust force with the potential to be increased by varying the load angle of the commutation.

In [5] the load angle is estimated for a rotational stepper motor in open loop operation by measuring the back-EMF and motor current. Transforming into frequency domain the load angle indirectly is yielded regarding the space vector representation. An additional motor and torque sensor applies the load torque. The drawback of application is that the torque must be measured to set the optimal load angle. In [6] a simulation of a rotational motor with a velocity controller and variable load torque is used to estimate an optimal load angle. However, sinusoidal commutation with constant load angle is not providing the maximum force for different velocities. The issue of phase lag with a closed loop controlled planar motor is solved by applying a phase advance time in [7], that can be regarded as linearly with velocity increasing load angle. Nevertheless, the optimal load angle can be in nonlinear relation to the velocity. Referring to the procedure of [8] the load angle is estimated without additional measurement cost and without knowledge about the drive system or rather a model. Due to the proportional relation of current amplitude and thrust force the optimal load angle is determined by the lowest current that is necessary for a desired motion. In other words, a higher force can be provided when using the same current amplitude at a certain velocity in comparison to a non-optimal load angle. This procedure is picked up in this work and combined with an automatic optimization process. Applying bracketing methods, the nonlinear relation of optimal load angle and velocity is obtained.

2. TEST RIG PLATFORM

2.1 Topology and function principle of LHSM

The LHSM is fundamentally built up by a mover and a stator, which has a length of 2 m. The stator is made of an iron body in which grooves are milled in to obtain the tooth structure that is charcteristic for the function principle. The distance from one groove to the next is called as tooth pitch period T_T. The mover is composed of a non-ferromagnetic frame in which two motor modules are integrated. The design of a motor module itself is shown in Figure 1. In order to separate the magnetic circuits, spacers are integrated between the three phases. The bottom

surface is characterized by a tooth structure as well. One phase consists of stacked and laminated iron sheet with a centered permanent magnet. Wires wound within the iron sheet represent a coil. Air bearings mounted in the frame ensure that the magnetic attraction force can be compensated. Besides getting loose, the mover is kept aligned to the stator cross axis by additional air bearings at the side faces of the U-shaped frame.

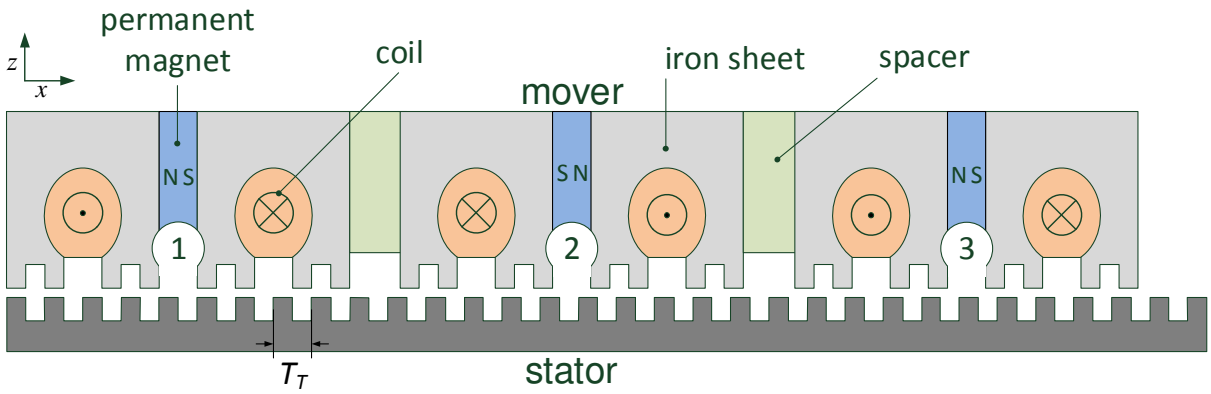

Figure 1: Design of the LHSM motor module.

The function principle corresponds to Sawyer's planar motor [9]. The mover permanent magnets provide a basic magnetic flux. Energizing the coils leads to an additional magnetic flux, which increases or decreases the permanent magnetic flux of the phases' legs. As a consequence, imbalanced reluctant forces of the legs result in a thrust. By half overlapping of the mover's and stator's teeth the maximum force roughly is achieved. Eventually, working with more than one phase and alternating current directions an approximately continuous horizontal thrust force is generated.

2.2 Test rig components

Beside the sinusoidal type LHSM, several components complete the test rig, which is presented in Figure 2.

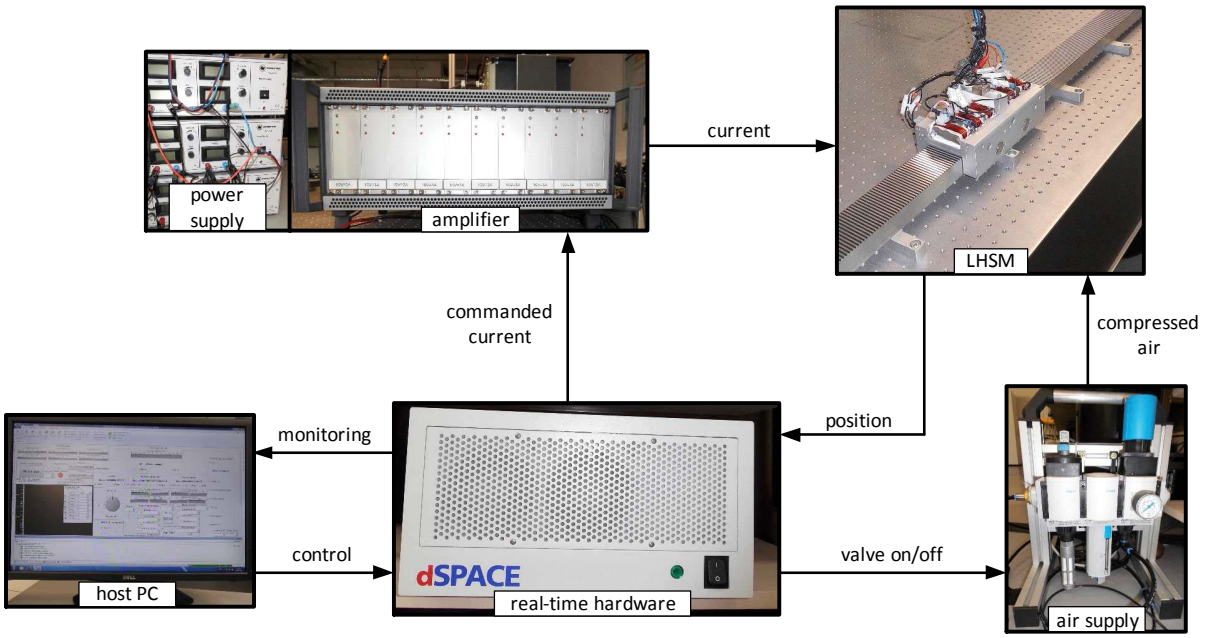

Figure 2: Test rig platform.

A power supply provides the electric energy with sufficient capacity for analog linear amplifiers. These are utilized to energize the coils for the two motor modules whose phases are arranged in a series connection. For the bearings, compressed air is provided by a stationary source. A preparation unit filters the compressed air from small particles and a switch valve allows turning on and off the air supply. In order to conduct closed loop operation a position feedback signal in terms of a magnetic incremental encoder is deployed. The measured data is acquired by a real-time hardware device. Moreover, that is responsible for commutation and outputs the command signals for the currents. Control algorithms and initialization processes are carried out as well with a sample rate of 20 kHz. A host PC is used to monitor the process with a graphical user interface and to give commands to the real-time hardware such as switching the control mode.

3. ALGORITHMICAL DETAILS

3.1 Principle functionality

Figure 3 shows the principle functionality of the automatic determination of an optimal load angle for a desired velocity. This block diagram is based on [8]. The motor will be operated current controlled by means of a velocity controller. At the beginning, the velocity for the optimal load angle to be estimated is defined as a set point of the velocity controller. As can be seen in Figure 4 (a), there exists a certain load angle at which the control signal $\hat{I}$ for the commutation is at a minimum. Regarding a reference load angle of 90° the optimal load angle is achieved by finding $\Delta\alpha_{opt}$ added to the reference value. At this point, the distance to the current limit is greatest whereby a maximum thrust force can be generated. To detect this optimal load angle bracketing methods will be used (see section 3.2).

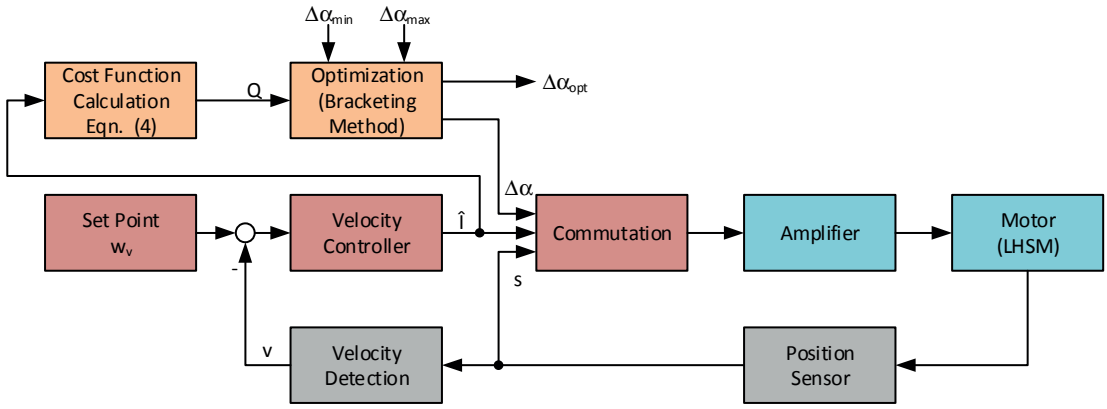

Figure 3: Block diagram for determination of an optimal load angle.

This optimal load angle must be determined for all interested velocities using the previously presented method. After that, a functional interrelation of $\Delta\alpha_{opt}=f(v)$ in terms of an analytical function or look-up table can be created using the individual results (see Figure 4 (b)).

3.2 Algorithms for derivate free optimization

To solve the one-dimensional optimization task, bracketing methods are used. These algorithms work without derivatives and find the minimum through iterative decreasing of the interval until the desired tolerance ε is achieved, in which the minimum lies. In this case, this is essential since there are no analytical solutions.

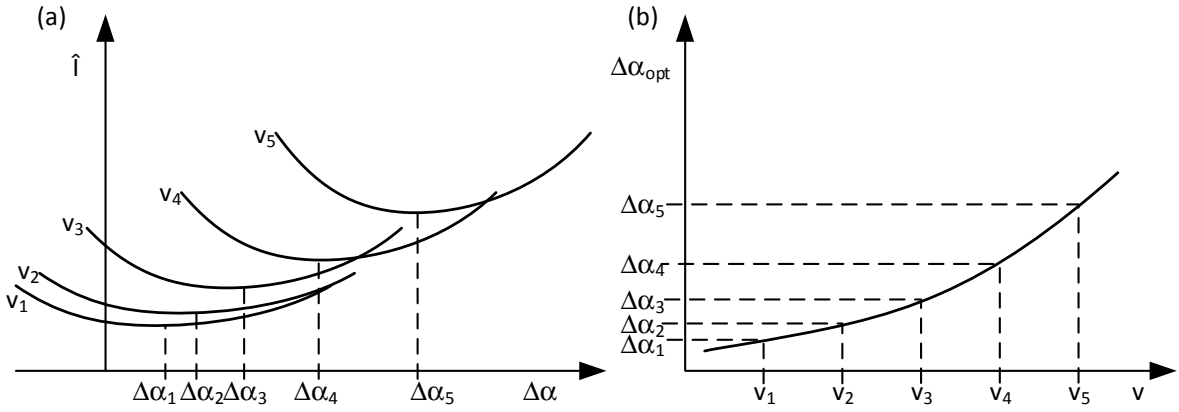

Figure 4: Interrelation (a) $\hat{I}$=f($\Delta\alpha$) and (b) $\Delta\alpha_{opt}$=f(v).

At the start of the search, an interval [$\Delta\alpha_{min}$, $\Delta\alpha_{max}$] wherein the optimal load value $\Delta\alpha_{opt}$ is presumed will be passed to the algorithm. In this application, Golden Section search [10], Fibonacci search [11] and Brent's method [12] are tested. These methods were also used in a previous research project, whereby Brent's method revealed the best performance [13]. The convergence of this algorithm is faster than for the other two algorithms, which leads to fewer cost function calls and thus saves time at the entire optimization process.

4. OPTIMIZATION PROCESS

4.1 Preliminary

The optimization process is based on the condition to manipulate the commutation function. Thus, the sinusoidal commutation characterized by the tooth pitch period T_T is modified by adding an additional phase angle $\Delta\alpha$. The position s_x determines the currents of the three phases yielding

$$\begin{aligned} i_1 &= \hat{I} \cdot \sin\left(\frac{2\pi}{T_z} \cdot s_x + \Delta\alpha \cdot \frac{\pi}{180}\right) \\ i_2 &= \hat{I} \cdot \sin\left(\frac{2\pi}{T_z} \cdot s_x + \frac{2}{3}\pi + \Delta\alpha \cdot \frac{\pi}{180}\right) \\ i_3 &= \hat{I} \cdot \sin\left(\frac{2\pi}{T_z} \cdot s_x + \frac{4}{3}\pi + \Delta\alpha \cdot \frac{\pi}{180}\right) \end{aligned} \tag{1}$$

with $\hat{I}$ as control signal or current amplitude respectively. The main objective is

$$\underset{\Delta\alpha_{opt}}{\mathrm{Min}}\left(Q(\hat{\mathbf{I}})\right) \tag{2}$$

whereby the time series of $\hat{I}$ at a constant velocity with starting index n_1 and ending index n_2 is used to determine a mean value at first:

$$\mathrm{mean}(\hat{\mathbf{I}}) = \frac{\sum_{k=n_1}^{n_2} \hat{I}_k}{n_2 - n_1} \tag{3}$$

Considering several runs at one load angle and squaring the mean value results in the following cost function

$$Q(\hat{\mathbf{I}}) = \sum_{k=1}^{N} mean(\hat{\mathbf{I}})^2 \tag{4}$$

with N as number of measurement runs.

4.2 Realization

For realization, a variable phase angle must be set at the ongoing operation. Furthermore, a script-based implementation enables the execution of the optimization process automatically. Once started at the host PC, load angles are optimized for a defined velocity range. Taking up the term load angle the delta-value is regarded in the following.

In order to explain the process one iteration cycle at one certain velocity is considered. The main parts of one iteration cycle are measurement run, data filtering, providing the cost function value and executing the optimization algorithm that adjusts the load angle for the next iteration.

Subsequently, the process shall be explained more precisely. Initially, the mover is positioned that way allowing a sufficient measurement range that especially is important at higher velocities. Following, the mode is switched from position to velocity control mode. In a separate work, the PID-controllers deployed were tuned model based. To verify the performance of the velocity control three different velocity steps are executed in forward and backward direction according to Figure 5. A sufficiently good transient behavior is achieved with a short settling time and little overshoot. Because of the LHSM's property, force fluctuations have an impact and are manifested to the measured velocity. Applying a filter reveals the steady velocity matching with the desired values.

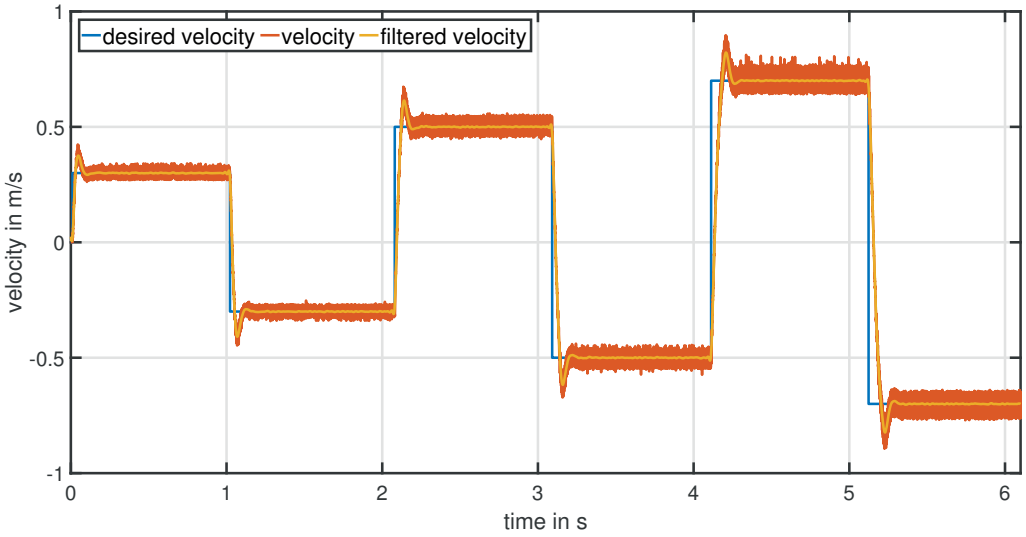

Figure 5: Velocity control for three different set points.

Setting a certain velocity the mover is driven forward and backward and the corresponding control signal is captured as time series in a data file. The control signal equals the current amplitude that is to be minimized. Since the current is marked with the impact of force fluctuations a filter is used as well to smooth the curve sufficiently and thus to reveal a transient response [14]. Due to acceleration and mass inertia, a high increase of the current can be seen in Figure 6 before reaching the steady state. Therefore, the interesting area is extracted by three steps. First, an upper and lower border around the filtered, steady state current is introduced. Afterwards, the overshoot is cut off by omitting the current until the border is exceeded for the last time. Finally, the first and the last part of the remaining current trajectory is cut off in order to avoid last small transient oscillations and filter impacts, respectively. The processed data is

saved and further measurement runs can be carried out. After that, the cost function value according to (4) is calculated. Including forward and backward direction yields

$$Q = Q_{forward} + Q_{backward} \tag{5}$$

The determined cost function value is used by the optimization algorithm in order to calculate an update of the load angle. Now, this new load angle is set within the commutation and the next iteration is executed according to the steps explained previously. The optimization run is terminated when the defined tolerance is achieved. Considering forward and backward measurements separately, the optimization process can be adopted to the directionality of the LHSM. In the next section, these and some other properties are discussed more in detail.

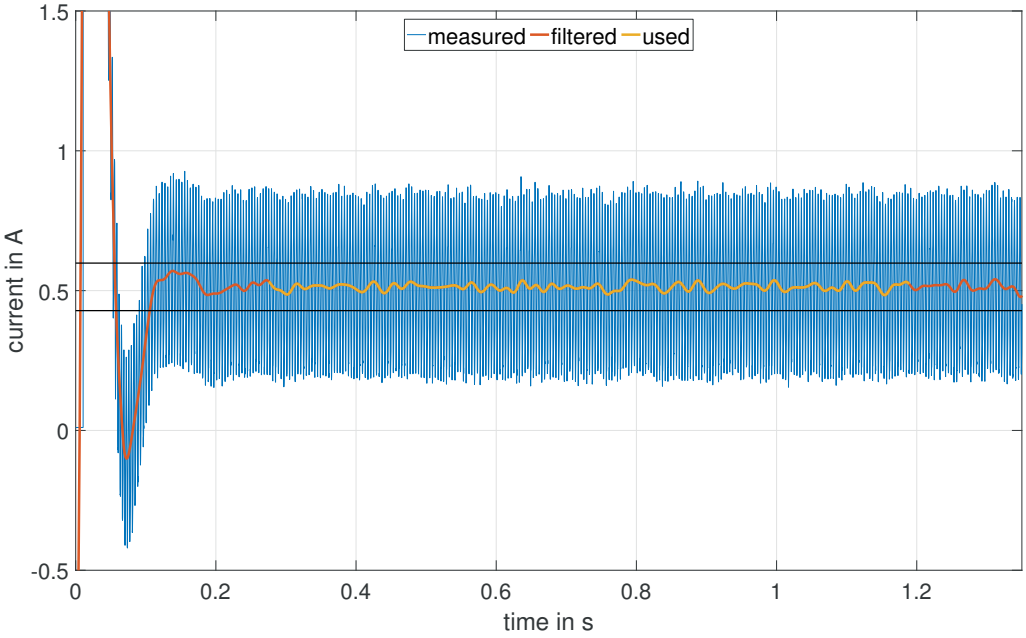

Figure 6: Filtering of current and section used to calculate the mean value.

5. RESULTS

5.1 Properties

Confirming the assumption to focus on Brent's algorithm according to section 3.2 Fibonacci and Golden Section search are used in real-time implementation as well.

In order to explore properties of these different methods 20 optimization runs for a velocity of 0.5 m/s are carried out. Only the positive moving direction making one measurement per iteration is regarded.

Initially, the convergence property is to be considered which can be evaluated by the number of iterations needed. For this reason, the average numbers are determined and shown in Table *I*. The result indicates that Brent's algorithm has the smallest number corresponding with lowest the optimization time.

To verify reproducibility, probability density functions (PDFs) are introduced. Therefore, mean values μ and standard deviations σ are calculated to determine the PDF according to:

$$P = f(\Delta\alpha_{opt}\,|\,\mu,\sigma) = \frac{1}{\sigma\sqrt{2\pi}}\, e^{\frac{-(\alpha_{opt}-\mu)^2}{2\sigma^2}} \tag{6}$$

Table I:
Comparison of examined optimization algorithms

	Optimization Algorithm		
	Brent	**Fibonacci**	**Golden Section**
Number of Iterations	18	25	25

Additionally, in order to examine whether the variance can be reduced the number of measurements is increased from one (*N=1*) to five (*N=5*) for the Brent search. The PDFs of the different methods are shown in Figure 7. At first, it should be noted that there is no reduction of variance, which can be rated by the width of the Gaussian curves representing the PDFs. Furthermore, the mean values are close to each other and it can be concluded that one measurement provides satisfying results yet. In contrast, Fibonacci and Golden section search show a deviating mean and a high variance represented by stretched Gaussian curves. In Table *II* the mean and standard deviation values of each method are indicated verifying the PDF curves.

The reason for the lower variance of Brent's algorithm can be explained by its working method. In addition to the bisection method, this algorithm also uses the secant method and inverse quadratic interpolation. The two latter ones include information of the function course to determine the next iteration points. This is leading to a good convergence and an accurate determination of the minimum in case of flat function courses existing in this application (see Figure 8). Thus, Brent's algorithm is used for the load angle optimization of the defined velocity range.

In general, there are systematic impacts explaining the relatively high variances. Considering the LHSM, different magnetization states of the stator affect the plant properties continuously. As well, vibrations of the mover have an influence to the force characteristic, since it is dependent on the vertical distance, i.e. the air gap between mover and stator. Further, less impacting causes for variances come from the real-time hardware and the power amplifier.

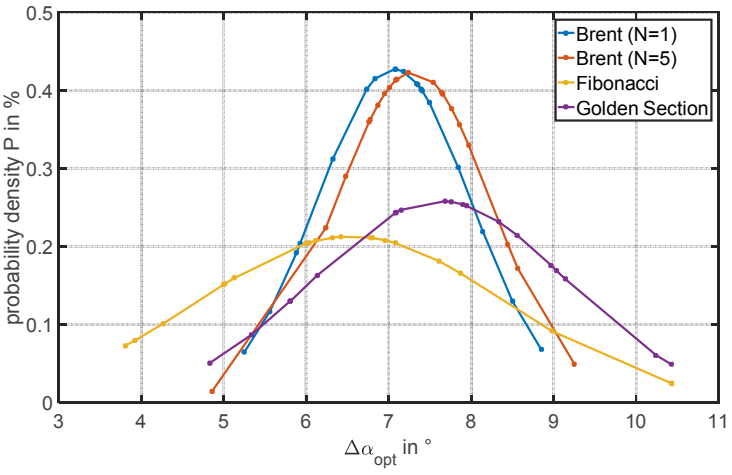

Figure 7: Probability density functions for examined approaches and distinction between one optimization (N=1) and five (N=5) measurement runs for Brent search.

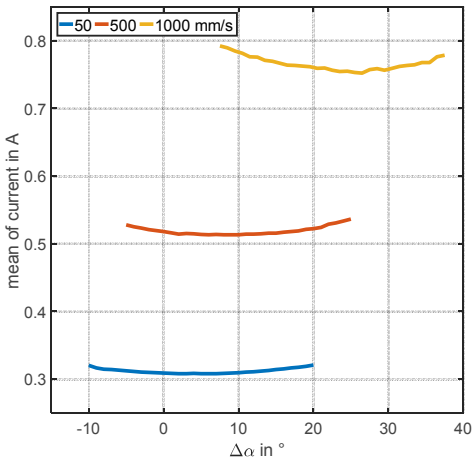

Figure 8: Detected curves $\hat{I}$ =f(Δα) for three different velocities.

Table II:
Statistical parameters of the examined methods

Method	Mean μ	Standard deviation σ
Brent (N=1)	7.0623	0.9334
Brent (N=5)	7.3024	0.9407
Fibonacci	6.5487	1.8724
Golden Section	7.6141	1.5447

5.2 Optimal load angle

Before starting the optimization, some configuration settings are done. At first, the number and values of the velocities being examined must be specified. To cover the range sufficiently while not increasing the runtime ten velocities are chosen. Additionally, an interval must be defined indicating the region the optimal load angle is located within. Extending the range too wide increases the number of iterations. Thus, by considering empirical values, the borders are set to ±30° for $\Delta\alpha_{opt}$.

After completing the configuration settings, the optimization of load angles over the defined velocity range carrying out forward and backward drive can be started. The procedure is executed automatically and lasts roughly half an hour until the optimal load angle of the last velocity is determined. As a result, a curve is obtained (see Figure 9) indicating a decrease of the load angle around 0 m/s and increase beyond velocities of 0.1 m/s. Due to the high gradient, equidistant velocities grid points are not recommended. Instead, a finer grid is considered to obtain a sufficiently smooth curve. Since the optimal load angle is determined including forward and backward direction the identified curve is mirrored along the zero axis.

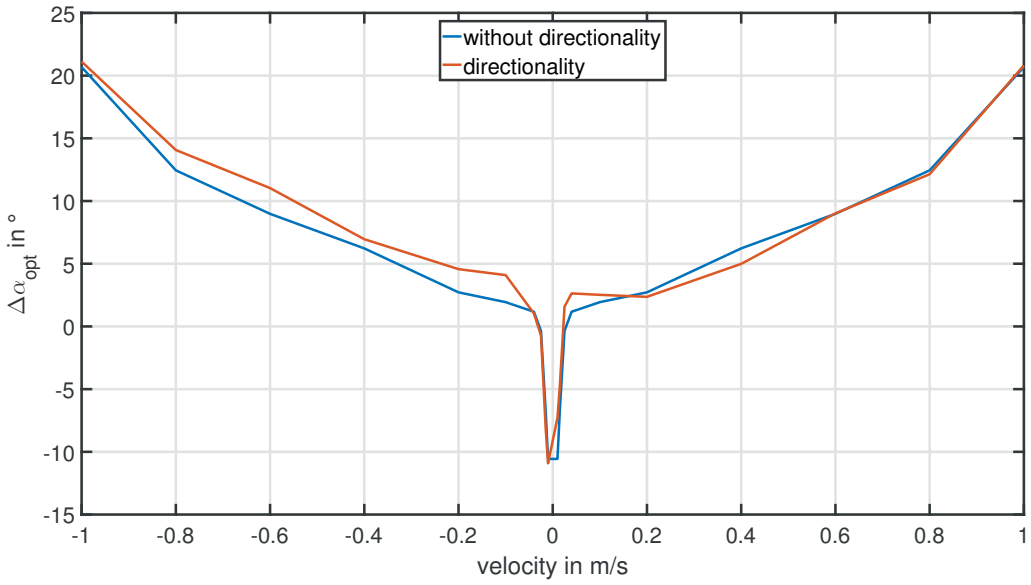

Figure 9: Optimal load angle curve.

However, due to special characteristics of the LHSM there are directional differences. Reasons for that are magnetic properties of the stator in terms of an offset shifted BH-characteristic. That means, in one direction there is existing more remanence flux than in the opposite one. Other reasons are constructive caused issues, e.g. considering not ideally arranged motor or phase modules. Moreover, the curvature of stator or mover surface may affect the air bearings in the way that a horizontal force component arises. Taking into account the directionality, an additional optimization run with ten positive and negative velocities is carried out consuming

twice the amount of time. The corresponding result is shown as well in Figure 9 exhibiting almost the same behavior at positive velocities. However, in negative domain a deviating characteristic can be regarded justifying the additional cost.

5.3 Validation

The obtained curves are implemented on the real-time system as look-up tables with the actual velocity as input providing $\Delta\alpha_{opt}$ for the commutation according to (1). To validate the results, the LHSM should realize velocity steps for both the constant load angle of 90° and the optimized load angle. Since the impact is significant at higher velocities, appropriate values are selected. As shown in Figure 10 (b) velocities of 0.8, 1 and 1.2 m/s are to be set successively in alternating direction. The first velocity is adjusted without differences but at the second step value a lower settling time reveals with the optimized execution. This is clarified at the current response outlined in Figure 10 (a) being less time in the limit of 5 A. The effect further intensifies at the last step in terms of not reaching the desired velocity value and not leaving the limit of the current when using the constant load angle

Comparing directional and directional free implementation, there are no rather significant differences that can be justified by the amount of the variance remembering Figure 7 so that no remarkable differences occur. Nevertheless, the optimized curve including directionality is used performing the validation because it meets the LHSM's properties better.

In summary, applying the optimized load angle characteristics at the commutation leads to amaximum thrust force and thus improved control behavior, especially at higher velocities.

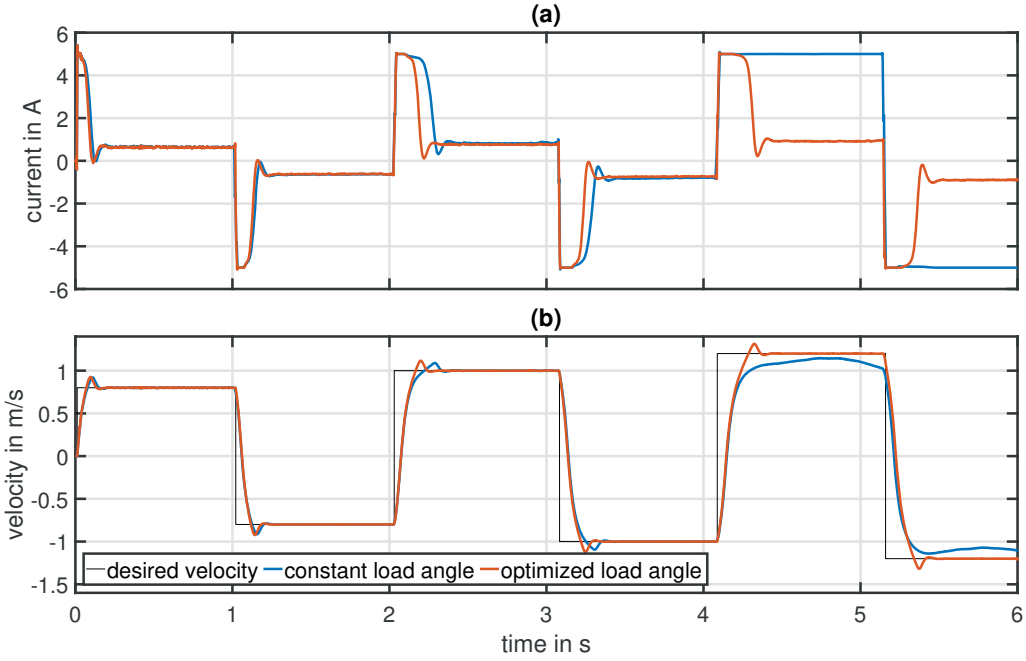

Figure 10: Velocity control with constant and optimized load angle.

6. CONCLUSIONS

In the presented work, an efficient procedure for load angle optimization was demonstrated and applied to a LHSM. This works without a model of the plant by minimizing the needed current when moving with a certain velocity. The optimization process is implemented on the real-time hardware and executed within velocity limits of the LHSM. Brent's algorithm provides the best

performance among other examined methods when optimizing one variable without any derivatives. Nonlinearity and directionality are captured and displayed in the load angle characteristic obtained by an automatic optimization process. Implemented as look-up table, the results show that load angle optimization is a useful opportunity to reduce the settling time and increase the maximum force available. The procedure presented can be applied to other sinusoidal motor types including rotational ones as well by low cost.

ACKNOWLEDGEMENTS

The authors would like to acknowledge the support of the German Ministry of Economics and Energy (BMWi) within the ZIM cooperation project (FKZ: KF2250120WD4).

REFERENCES

[1] A. Cassat, N. Corsi, R. Moser and N. Wavre: "DIRECT LINEAR DRIVES: Market and Performance Status", In: LDIA2003, Proceedings of the 4th International Symposium on Linear Drives for Industry Applications, Birmingham, UK, September 8-10, 2003.

[2] Muhammend F. Rahman and Aun-Neow Poo: "An Application Oriented Test Procedure for Designing Microstepping Step Motor Controllers", In: IEEE Transactions on Industrial Electronics, Vol. 35, No. 4, pp. 542-546, 1998.

[3] R. Welch and G. Kaufman: "Advantages of Sinusoidal Ke Motor over the Quasi-sinusoidal Ke Motor when operated with a Trapezoidal Drive", In: Proceedings of the third Annual Motion Control Technology, pp. 121-128, Orlando, USA, 2008.

[4] C. Röhrig: "Optimal Commutation Law for Three-Phase Surface-Mounted Permanent Magnet Linear Synchronous Motors", In: Proceedings of the 45th IEEE Conference on Decision & Control, pp. 3996-4001, Boston, USA, 1991.

[5] S. Derammelaere, F. Verbelen and K. Stockman: "Robust sensorless load angle control for stepping motors", In: 18th International Conference on Electrical Machines and Systems (ICEMS), Pattaya, Thailand, 2015.

[6] G. Eisenbeis: „Einige Aspekte beim Vergleich von Synchronmotor-Positionier-Antrieben mit Elektronischer Kommutierung bei Fremd- und Selbsterregung", Kaiserslautern, 1997.

[7] A. E. Quaid, Y. Xu and Ralph L. Hollis: "Force characterization and commutation of planar linear motors", In: IEEE ICRA Proceedings, Albuquerque, USA, 1997.

[8] M. Eichhorn: "Gebrauchsmusterschrift DE 299 14 972 U1", Ilmenau, 1999.

[9] E. R. Pelta: „Two-Axis Sawyer Motor for Motion Systems", In: IEEE Control Systems Magazine, Volume 7, Issue 5, pp. 20-24, 1987.

[10] J. Kiefer, "Sequential minimax search for a maximum," Proceedings of the American Mathematical Society, vol. 4, 1953, pp. 502-506.

[11] D.E. Ferguson, "Fibonaccian searching," Communications of the ACM, vol. 3, no. 12, 1960, pp. 648.

[12] R. P. Brent: „Algorithms for Minimization without Derivatives", Prentice-Hall, Mineola, 2013. -ISBN: 978-0-486-41998-5.

[13] M. Eichhorn, H.C. Woithe, and U. Kremer: Comparison of Guidance Modes for the AUV “Slocum Glider” in Time-Varying Ocean Flows - Oceans '14 IEEE Taipei, Taipei, Taiwan, 2014,

[14] F. Gustafsson: „Determining the Initial States in Forward-Backward Filtering”, In: IEEE® Transactions on Signal Processing, Vol. 44, pp. 988–992, 1996.

CONTACTS

M. Sc. Heiko Weiß heiko.weiss@tu-ilmenau.de
Thomas Bauer t.bauer@tu-ilmenau.de
Dr. Mike Eichhorn mike.eichhorn@tu-ilmenau.de